Mater. Res. Soc. Symp. Proc. Vol. 1055 © 2008 Materials Research Society 1055-GG13-02

Near infrared intersubband absorption in cubic GaN/AlN superlattices

Eric A. DeCuir, Jr. [1], Emil Fred[1], Omar Manasreh[1], Jorg Schormann[2], Donat J. As[2], and Klaus Lischka[2]
[1]Department of Electrical Engineering, University of Arkansas, 3217 Bell Engineering Center, Fayetteville, AR, 72701
[2]Department of Physics, University of Paderborn, Warburger Srasse 100, Paderborn, 33095, Germany

ABSTRACT

Room temperature near-infrared intersubband transitions were observed in MBE grown non-polar cubic GaN/AlN superlattice structures. The peak wavelengths of these transitions were observed in the spectral region of 1.5–2.0 μm and were theoretically supported using a transfer matrix approach. All samples were unintentionally doped and grown on 3C-SiC substrates with a 100 nm GaN buffer. Each structure consisted of a 20 periods of GaN/AlN superlattice capped with 100nm of GaN. The thickness of the AlN barrier was fixed at 1.35, while the thickness of the GaN well was varied between 1.6 and 2.1nm. Electrochemical Capacitance Voltage (ECV) measurements allowed direct measurement of the intrinsic carrier concentration in a thick unintentionally doped cubic GaN layer, which confirmed sufficient population of the ground state energy level.

INTRODUCTION

The polar nature of the hexagonal III-nitrides [1] grown on the c-plane (0001) sapphire contributes to the presence of strong intrinsic piezoelectric and pyroelectric fields at hetero-interfaces. The presence of these sheet charges at hetero-interfaces have been shown to influence optical and electrical properties, thereby making the design of intersubband based devices problematic [2-3]. In the past, efforts to reduce or eliminate these effects have been accomplished by using R-plane (10-12) sapphire substrates which result in non-polar A-plane (11-20) hexagonal nitride material, thus effectively eliminating the contributions of these large electric fields [4-5]. However, the excellent crystal symmetry exhibited by the non-polar cubic III-nitride system also provides a means to circumvent the challenging effects of sheet charges at hetero-interfaces.

The availability of a large conduction offset (~1.33eV) in the cubic system consisting of AlN and GaN allows intersubband absorption tuning over a wide spectral. In this study, it is the magnitude of this band offset that has enabled the tuning of intersubband absorption wavelengths near the important telecommunication wavelength of 1.55μm. Great strides in understanding the growth kinetics of cubic nitride materials [6] has enabled the growth of high quality cubic GaN/AlN superlattices giving rise to near-infrared intersubband absorption first reported in the cubic nitride system [7].

EXPERIMENT

In this study, all structures were grown at 720 °C on free standing 3C-SiC (001) substrates by plasma assisted molecular beam epitaxy using growth techniques as described in reference 6. The structures consisted of a 100 nm thick cubic GaN buffer, followed by a 20 period GaN/AlN superlattice (SL), and finished with a 100 nm thick cubic GaN cap. For the three samples reported, the barrier thicknesses were fixed at 1.35 nm for all samples while the well thickness was altered in the range of 1.6 - 2.1 nm. Further details about the growth of these superlattices may be found in reference 7.

Optical absorption due to intersubband transitions was observed in non-polar cubic GaN/AlN short period superlattices grown by plasma assisted molecular beam epitaxy on 3C-SiC substrates. Since absorption in quantum well structures occurs only for polarization parallel to the growth axis (z-axis) and is forbidden under normal incidence, a waveguide configuration is used to enhance electron-photon coupling by taking advantage of multiple passes of light. The waveguide geometry used consisted of two parallel facets polished at 45^{o} to allow multiple light passes through the active region. The peak positions of the intersubband transitions obtained at room temperature were observed in the spectral range of 1.5 to 2 μm. These peak absorption energies observed in experiment were further supported by using a transfer matrix method (also known as a propagation matrix method) to calculate the bound state energy levels in these quantum wells.

RESULTS AND DISCUSSION

All optical absorption measurements were recorded using a Bruker Fourier-transform 125HR spectrometer. The configuration consisted of a quartz-halogen light source, an InSb cooled detector, and a calcium fluoride beam-splitter. This configuration permitted measurements in the spectral range of one-three microns. A transfer matrix method as described by Levi [8] was used to calculate the bound state energy levels as a function of well width. These calculated values are then compared to the peak position energies obtained from the optical absorption spectra of the intersubband transitions. Furthermore, ECV measurements were used to quantify the carrier concentrations in these quantum wells to ensure sufficient ground state population.

The room temperature absorbance spectra of the intersubband transition in three superlattice samples are plotted in Fig. 1. In these figures, the absorbance is defined as the product of the absorption coefficient (α) and the total thickness of the quantum wells (active region) in the superlattice (L). In these superlattices, it is expected that splitting of the energy levels occur due to overlap between localized wave functions in neighboring quantum wells, which leads to the formation of mini-bands. It is expected that the presence of these minibands may contribute to the inhomogenous broadening of the transitions; however, this broadening is negligible as compared to the inhomogenous broadening introduced by well fluctuations [9]. Homogenous broadening of the transition line shape is commonly described by a Lorentzian lineshape whose FWHM may also attributed to the dephasing time of excited electrons (associated with electron-electron scattering processes) [10-11]. Consequently, a dual Lorentzian fit has been shown to elucidate the assymetrical line shape revealed in Figure 1. While the line-shape of spectra B and C nearly approach that of a single Lorentzian, the

asymmetrical line shape of sample A is best fitted by two Lorentzian functions as seen in Fig. 1 (dotted lines). Also, the absorbance peak of sample C covers the wavelength of 1.55 μm, which is a common optical communication wavelength due its low attenuation in silica fibers. As summarized in Table I, it can be seen the full width at half maximum (FWHM) of each absorption peak is as much as five times broader as compared to the FWHM of the intersubband transitions in other systems, such as GaAs/AlGaAs and hexagonal AlN/GaN [12, 13]. This lapse in crystal quality is linked to the metastable nature of cubic-nitride system which lends additional obstacles in maintaining high crystal qualities as exhibited by the stable hexagonal counterpart. However, this first time observation in the cubic system further demonstrates the potential for using cubic GaN/AlN superlattices for near infrared optical detectors while avoiding the spontaneous polarization effects seen in the hexagonal system.

Table I. Summary of the 20-period cubic-GaN/AlN superlattice samples used in the present study. FWHM is the full width at half maximum of the intersubband transition spectra, n_{2D} is the two dimensional electron gas obtained by electrochemical capacitance measurements, and E_F is the Fermi energy level calculated from Eq. (1).

Sample	**Well Width(nm)**	**Peak Energy (meV)**		**FWHM (meV)**	**n_{2D} ($10^{11}cm^{-2}$)**	**E_F (meV)**
		Measured	**Calculated**			
A	2.1	620	630	182	2.79	3.52
B	1.75	696	734	211	2.33	2.94
C	1.6	751	781	219	2.13	2.68

To further confirm the observation of intersubband transitions in these superlattices, a comparison between the experimental data and the calculated results obtained via a transfer matrix calculation is given in Fig. 2. The experimental data (represented by solid circles) were obtained directly from the peak position of the absorbance spectra while the calculated data (blue line) is obtained by taking the difference between the ground state (E_1) and the first excited state (E_2). The calculations were made for an electron effective mass of $0.19m_o$, where m_o is the free electron mass [14]. In this transfer matrix approach, the experimental values are in reasonable agreement with the calculated trend of the $E_1 \rightarrow E_2$ transition energy considering the simplistic model used in this study does not take into account many-body or conduction band non-parabolicity effects [10]. The most significant parameters which enter this calculation are the electron effective masses in the cubic-GaN well region and the ratio between the conduction and valence bands offsets (ΔE_{CV}). The best agreement between the experimental data and calculated results shown in Fig. 2 was found using a conduction band offset (ΔE_{CV}) of 70:30. While ΔE_{CV} has not been thoroughly investigated for cubic III-nitrides, the ratio used here (70:30) is in accordance to those reported for the hexagonal III-nitrides [15]. A summary of the experimental and calculated results are given in Table I.

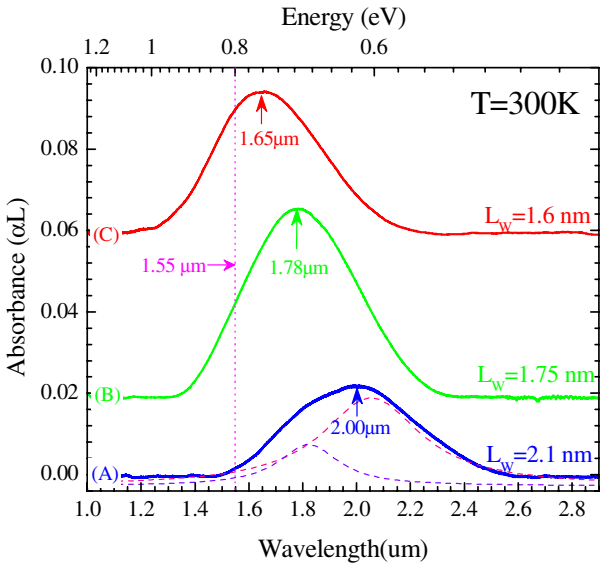

Figure 1: Room temperature absorbance spectra of intersubband transitions measured for three cubic GaN/AlN superlattice samples with different well thicknesses (solid lines). Dual Lorentzian fit for the absorbance spectra of sample C (dotted lines)

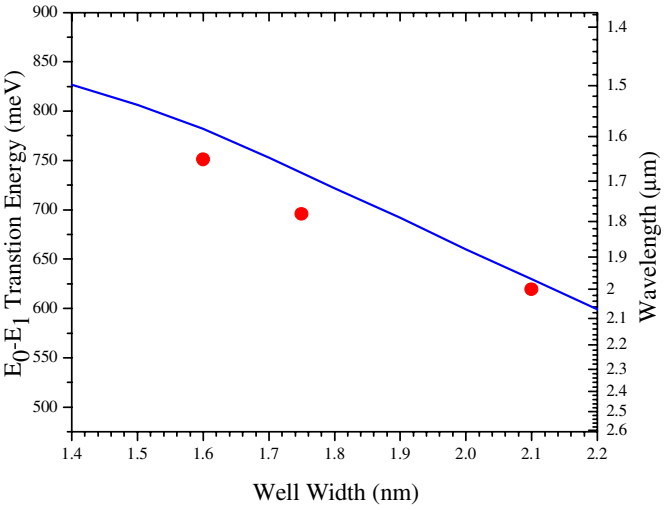

Figure 2: Peak position energies of intersubband transitions in cubic GaN/AlN superlattices (solid circles) and calculated (blue line) as a function of well width.

The charge carrier concentrations were measured using an electrochemical capacitance-voltage profiler (ECVPro). Since etching AlN is not possible due to the fact that the ultraviolet source used in the ECVPro system does not cover the band gap of AlN, a reference sample with a thick cubic GaN layer was grown under identical growth conditions as those of the GaN/AlN superlattices. This reference layer was tested using the ECVPro system and the results are shown in Fig. 3.

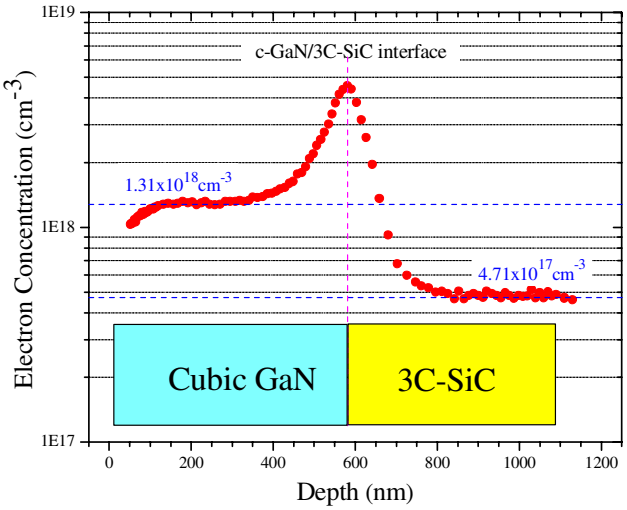

Figure 3: Electron concentration in a reference thick cubic GaN layer as a function of etch depth using an electrochemical capacitance-voltage (ECV) profiler.

It is clear from this figure that the bulk carrier concentration (N_{3D}) as a function of the etched depth is on the order of $1.31 \times 10^{18} cm^{-3}$. The peak observed at the depth of ~580 nm is due to the charge accumulation at the GaN/SiC interface. The carrier concentration of $4.71 \times 10^{17} cm^{-3}$ observed in the SiC substrate is in good agreement with the values provided by the manufacturer of the substrate.

By using the measured three-dimensional carrier concentration of unintentionally doped cubic-GaN and the well widths determined from RHEED oscillation and confirmed by the high resolution X-ray diffraction measurements, the Fermi energy level (E_F) position in the superlattices is calculated using the following expression [16]:

$$E_F \approx E_o + n_{2D} \pi \hbar^2 / m^*, \quad (1)$$

where n_{2D} is the two-dimensional electron concentration, ħ is Planck constant, and m^* is the effective mass. The calculated values of E_F for three samples are listed in Table I. Since the well width is small and the effective mass in relatively large, the calculated Fermi energy level is slightly above the ground state. Nonetheless, this condition is sufficient for population of the ground state with electrons, which is a necessary condition to observe intersubband transitions.

CONCLUSIONS

In conclusion, intersubband transitions were observed in the near-infrared spectral region in cubic-GaN/AlN short period superlattices grown on cubic SiC substrates. Growth enhancement of cubic nitride has enabled the observation of intersubband transitions in this system in the absence of piezoelectric effect. The electrochemical capacitance-voltage measurements confirm the presence of relatively high carrier concentrations in the cubic GaN system investigated here. Good agreement between the experimental and calculated peak energy position of the intersubband transition is obtained. The optical absorption measurements confirm the tuning of the intersubband transition in cubic GaN/AlN to the near infrared spectral region. In particular, the peak position of the intersubband transition spectrum reached the 1.55 μm spectral region, which is an important wavelength used in optical communications.

ACKNOWLEDGMENTS

The work at the University of Arkansas was funded by the Air Force Office of Scientific Research (Program Manager: Dr. Gernot Pomrenke) and by the Arkansas Science & Technology Authority. We would also like to thank H. Nagasawa and M. Abe from SiC Development Center, HOYA Corporation, for supplying the 3C-SiC substrates.

REFERENCES

1. F. Bernardini, V. Fiorentini, and D. Vandenbuilt, *Phys. Rev*. B **56**, R10024(1997).
2. O. Ambacher, R. Dimitrov, M. Stutzmann, B. E. Foutz, M. J. Murphy, J. A. Smart, J. R. Shealy, N. G. Weimann, K. Chu, M. Chumbes, B. Green, A. J. Sierakowski, W. J. Schaff, and L. F. Eastman, *Physica Status Solidi* B **216**, 381(1999).
3. Seoung-Hwan Park and Shun-Lien Chuang, *Appl. Phys. Lett*. **76**, 1981 (2000).
4. C. Gmachl and H. M. Ng*, Electron. Lett.* **39**, 567(2003).

5. E. Kuokstis, W. H. Sun, C. Q. Chen, J. W. Yang, and M. A. Khan, *J. Appl. Phys.* **97**, 103719(2005).
6. J. Schormann, S. Potthast, D. J. As, and K. Lischka, *Appl. Phys. Lett*. **90**, 41918 (2007).
7. E. A. DeCuir, Jr, E. Fred, M.O. Manasreh, J. Schörmann, D. J. As, and K. Lischka. *Appl. Phys. Lett.* **91**, 041911(2007)
8. A. F. J. Levi, Applied Quantum Mechanics (Cambridge University Press, Cambridge, 2003), Chap. 4, p. 167.
9. T. Asano and S. Noda. *Jpn. J. Appl. Phys*. **37** 6020(1998).
10. . M. Tchernycheva, L. Nevou, L. Doyennette, F. H. Julien, E. Warde, F. Guillot, E. Monroy, E. Bellet-Amalric, T. Remmele, and M. Albrecht, *Phys. Rev. B* **73**, 125347(2006).
11. N. Iizuka, K. Kaneko, and N. Suzuki. *J. Appl. Phys*., Suppl. **81**, 1803 (2002).
12. K. K. Choi, B. F. Levine, R. J. Malik, J. Walker, and C.G. Bethea, *Phys. Rev*. *B* **35**, 4172(1987).
13. F. H. Julien, M. Tchernycheva, L. Nevou, L. Doyennette, R. Colombelli, E. Warde1, F. Guillot, and E. Monroy. *phys. stat. sol. (a)* **204**, 1987 (2007).
14. K. Kim, W. R. L. Lambrecht, B. Segall, and M. Van Schilfgaarde, *Phys. Rev*. *B* **56**, 7363(1997).
15. I. Vurgaftman, J. R. Meyer and L. R. Ram-Mohan, *J. Appl. Phys.* **89**, 5815(2001).
16"*Semiconductor heterojunctions and nanostructures*", M. O Manasreh, (McGraw-Hill, New York , 2005), p. 174.